

# White Electroluminescent Single-Polymer Achieved by Incorporating Three Polyfluorene Blue Arms into a Star-Shaped Orange Core

Lei Chen,<sup>1,2</sup> Pengcheng Li,<sup>1,2</sup> Hui Tong,<sup>1</sup> Zhiyuan Xie,<sup>1</sup> Lixiang Wang,<sup>1</sup>  
Xiabin Jing,<sup>1</sup> Fosong Wang<sup>1</sup>

<sup>1</sup>State Key Laboratory of Polymer Physics and Chemistry, Changchun Institute of Applied Chemistry, Chinese Academy of Sciences, Changchun 130022, People's Republic of China

<sup>2</sup>Graduate School of Chinese Academy of Sciences, Beijing 100039, People's Republic of China

Correspondence to: L. X. Wang (E-mail: lixiang@ciac.jl.cn) or H. Tong (E-mail: chemtonghui@ciac.jl.cn)

Received 12 January 2012; accepted 12 March 2012; published online

DOI: 10.1002/pola.26061

**ABSTRACT:** A series of star-like dopant/host single-polymer systems with a D-A type star-shaped orange core and three blue polyfluorene arms were designed and synthesized. Through tuning the doping concentration of the orange core and thermal annealing treatment of white polymer light-emitting diodes based on them, highly efficient white electroluminescence has been achieved. A typical single-layer device (ITO/PEDOT:PSS/polymer/Ca/Al) realized pure white emission with a luminous efficiency of 16.62 cd A<sup>-1</sup>, an external quantum efficiency of 6.28% and CIE coordinates of (0.33, 0.36) for S-WP-

002TPB3 containing 0.02 mol % orange core. The high efficiency of the devices could be mainly attributed to the suppressed concentration quenching of the dopant units, more efficient energy transfer from polymer host to orange dopant and thermal annealing-induced  $\alpha$ -phase polyfluorene (PF) self-dopant in amorphous PF host. © 2012 Wiley Periodicals, Inc. *J Polym Sci Part A: Polym Chem* 000: 000–000, 2012

**KEYWORDS:** benzothiadiazole; branched; conjugated polymers; light-emitting diodes; white electroluminescence

**INTRODUCTION** White organic light-emitting diodes (WOLEDs) have attracted widely research interest,<sup>1</sup> as their potential applications in full-color flat displays, back light of liquid crystal displays, and solid-state illumination sources. Compared to WOLEDs based on small-molecule emitters, white polymer light-emitting diodes (WPLEDs) show huge advantages in low cost, large area, and flexible displays, as they could be easily fabricated using solution-manufacturing process. After nearly two decades' effort, several strategies have been presented to achieve WPLEDs, such as multiple emissive layer device systems,<sup>2</sup> single emissive layer polymer-blend systems,<sup>3</sup> and single-polymer systems.<sup>4</sup> Although the interfacial mixing of different layers and serious bias-dependent electroluminescent (EL) spectra limit the applications of multilayer-device systems, WPLEDs based on polymer-blend systems have achieved great progress in device efficiency. Among them, for fluorescent material systems, Yang group reported two-color simultaneous WPLEDs with a luminous efficiency (LE) of 17.9 cd A<sup>-1</sup>,<sup>5</sup> Cao et al.<sup>6</sup> illustrated a three-color WPLED with a LE of 14.0 cd A<sup>-1</sup>. Using phosphorescent dyes, several groups have realized a LE more than 30.0 cd A<sup>-1</sup> for two-color phosphorescent WPLEDs.<sup>7</sup> The most efficient three-color phosphorescent WPLEDs was reported by Cao et al.<sup>8</sup> with a LE of 24.3 cd

A<sup>-1</sup>. Nevertheless, the disadvantage of intrinsic phase separation of different chromophores in polymer-blend systems affects the device efficiency and life-time for long-term operation. This problem could be avoided through covalently attaching chromophores to polymer host to develop single-polymer systems. At the early stage, WPLEDs based on single-polymer systems were mainly demonstrated with blue-light emission from blue dopant and orange-light emission from its aggregation/excimer/electromer.<sup>4</sup> However, this kind of white electroluminescence usually show low efficiency, as the formation of aggregate/excimer/electromer induces to low radiative decay rates of excitons.

Our group has proposed a new strategy to develop two- or three-color white light emitting single-polymers by incorporating an orange emitter or both a green fluorophore and a red fluorophore to a blue light emitting polymer host.<sup>9</sup> Compared to corresponding polymer-blend system, WPLEDs based on these single-polymer systems show higher EL efficiency and more stable bias-independent EL spectra.<sup>10</sup> Besides, the intrinsic phase separation could be avoided due to the chemical molecular dispersion feature, so that longer device operation life-time is expectable. By enhancing the fluorescent quantum efficiency ( $\phi_f$ ) of the dopant unit,<sup>11</sup> covalently attaching the dopant to the side chain of the blue host,<sup>12</sup> introducing blue

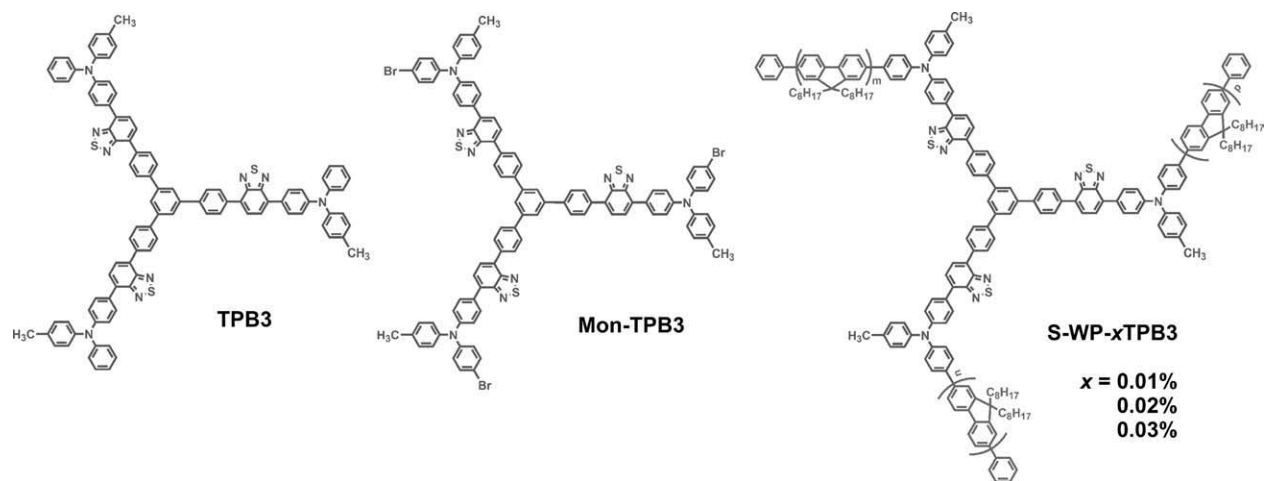


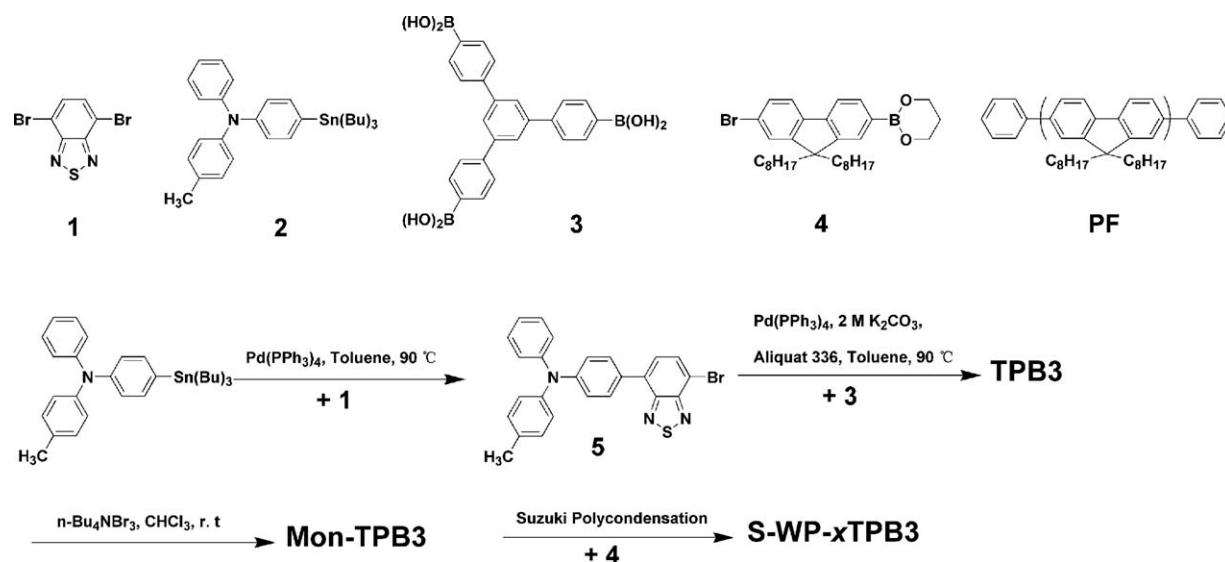
**CHART 1** Chemical structure of TPB3, Mon-TPB3 and S-WP-xTPB3.

dopants to improve the efficiency of the blue species,<sup>13</sup> the EL efficiencies of the devices based on single-polymers were successively improved to 12.8 cd A<sup>-1</sup> and 8.6 cd A<sup>-1</sup> for single-layer two- and three-color WPLEDs. The LE of them could be further improved to 16.9 and 15.4 cd A<sup>-1</sup>, respectively, by introduction of additional alcohol soluble electron-injection layers.<sup>14</sup> Recently, these approaches also have been adopted in several single-polymer systems reported by other groups. For instance, Cao et al.,<sup>15</sup> Shu et al.,<sup>16</sup> Shim et al.,<sup>17</sup> Hsu et al.,<sup>18</sup> Chen et al.,<sup>19</sup> and Chow et al.<sup>20</sup> have succeeded in realizing WPLEDs based on single-polymer systems. Through covalently incorporating fluorescent green emitting 2,1,3-benzothiadiazole (BT) units and a phosphorescent red emitting osmium complex into the backbone of PF, Shu et al.<sup>21</sup> developed a white electrophosphorescent single-polymer with a LE of 10.7 cd A<sup>-1</sup>, ranked as one of the highest values reported so far for white emitting single-polymers by simultaneously using both singlet and triplet excitons. In general, WPLEDs based on single-polymer systems show suppressed intrinsic phase separation and bias-independent EL spectra, but lower efficiency compared with those devices based on polymer-blend systems containing phosphorescent dyes. Thus, we have to develop new white EL single-polymer materials with improved efficiency.

In our previous work, most of the dopants were linear D-A type molecules. They severely suffer from concentration quenching<sup>22</sup> due to the strong intermolecular interactions in solid state, which will lead to low EL efficiency.<sup>23</sup> Thus, we believe that the inhibition of the concentration quenching of dopant units will be beneficial for improving EL efficiency of WPLEDs based on single-polymer systems with “dopant/host” feature. Star-shaped molecules and polymers have recently attracted widely research interests due to their unique molecular structures and optoelectronic properties.<sup>24</sup> Especially, their highly branched and globular features will be helpful for eliminating the intermolecular interaction and concentration quenching. For example, Huang et al.<sup>25</sup> have reported a set of fluorene-based six-armed nanostar macromolecules. They show greatly improved solid-state  $\phi_f$  (around 0.90) compared to that of linear PF (0.55).<sup>26</sup> Very

recently, we reported a series of star-like single-polymers through incorporating six PF arms in a star-shaped orange core (1,3,5-tris(4-(7-(4-(*N,N*-diphenylamino)phenyl)-2,1,3-benzothiadiazole-4-)phenyl)benzene, TPB6).<sup>27</sup> The concentration quenching of the orange dopants in these polymers could be completely suppressed in the doping range. The single-layer devices based on these polymers realized highly efficient white electroluminescence with an external quantum efficiency (EQE) of 6.36% and a LE of 18.01 cd A<sup>-1</sup>. However, the TPB6 unit is difficult to synthesize and purify in large amount due to its relatively poor solubility, which greatly limits its further application.

In this article, by introduction of three methyl groups to TPB6 unit, we designed a star-shaped orange core (TPB3, see in Chart 1) with improved solubility. TPB3 and its corresponding A<sub>3</sub> type brominated comonomer could be obtained much easier compared with TPB6 and its A<sub>6</sub> type comonomer. Moreover, the single-polymers achieved by incorporating three PF arms into TPB3 orange core also show high EL efficiency. We ascribed the high efficiency to the following three aspects: (1) By introduction of a star-shaped orange core to build star-like polymers with three blue PF branching arms, the concentration quenching effect of the orange dopant units could thus be efficiently suppressed. (2) Blue-shifted absorption band of the orange dopant compared to previously used linear orange dopant<sup>11</sup> would lead to superior Förster energy transfer from PF host to the dopant and the appropriate orange emission wavelength with almost the strongest human eye response was beneficial for improving the brightness, LE, and power efficiency (PE) of the polymer light-emitting diodes (PLEDs). (3) Formation of  $\alpha$ -phase PF self-dopant in amorphous PF host through thermal annealing treatment of the devices could greatly enhance the blue emission part. As a result, white electroluminescence with simultaneous blue emission (436/460 nm) and orange emission (560 nm) was obtained. The best single-layer device of the star-like polymers achieved a high LE of 16.62 cd A<sup>-1</sup> and an EQE of 6.28% with Commission Internationale de L'Eclairage (CIE) coordinates of (0.33, 0.36). The LE and EQE



SCHEME 1 Synthetic routes of star-shaped orange dopant and polymers.

value of the three-arm polymer are comparable to those of six-arm polymers but almost twice that of the linear orange molecule doped polymers.<sup>11,23b</sup>

## RESULTS AND DISCUSSION

### Design and Synthesis

Scheme 1 illustrates the chemical structure of orange dye and polymers. We designed a (DA)<sub>3</sub>D' type orange dye because it is beneficial for reducing their concentration quenching effect in solid state mainly due to the intermolecular dipole-dipole interactions. First, compared to corresponding D-A type molecules, D-A-D' type molecules possess a pair of antiparallel dipoles, thus the dipole-dipole interaction of them is weaker.<sup>22,28</sup> Second, star-shaped molecular architecture could further suppress the intermolecular interaction of the dopants.<sup>24</sup> We selected 2,1,3-benzothiadiazole unit as the electron acceptor, as its derivatives are of high Φ<sub>f</sub>.<sup>28</sup> (4-Methyl-phenyl)-diphenyl-amine and 1,3,5-triphenylbenzene (TPB) were chosen to be the peripheral electron-donating group and central unit, respectively. As a result, we obtained a star-shaped orange model compounds (MCs) with high Φ<sub>f</sub>, named as TPB3. PF was used as the branching arms because of its blue emission, high Φ<sub>f</sub> in solid state, and good charge-carrier transport properties.<sup>29</sup> By incorporating three PF blue arms into the star-shaped orange core, we obtained a star-like single-polymer system. More branched arms are also favorable for weakening the concentration quenching effect of the dopant.

The synthetic routes of the orange MC (TPB3), monomer and polymers are also shown in Scheme 1. Bromination of TPB3 with *n*-(C<sub>4</sub>H<sub>9</sub>)<sub>4</sub>NBr<sub>3</sub>, we afforded its A<sub>3</sub> type monomer,

Mon-TPB3. Star-shaped polymers were synthesized by Suzuki polycondensation with an AB type 9,9-dioctylfluorene monomer and A<sub>3</sub> type orange dopant monomer. The doping concentration of TPB3 was controlled to be 0.01, 0.02, and 0.03% to tune the relative intensity of the blue emission and orange emission. The polymers are recorded as S-WP-xTPB3, where *x* denotes the percentage content of TPB3.

### Properties of Orange Dopant

The photophysical, electrochemical, and thermal properties of TPB3 were studied, their corresponding values are listed in Table 1. The absorption and photoluminescent (PL) spectra in dilute toluene solution of TPB3 are shown in Figure 1. The absorption (λ<sub>abs</sub>) and emission (λ<sub>em</sub>) peaks of TPB3 are at 452 and 572 nm, respectively. The absorption spectrum of the linear orange dopant we previously used, 4,7-bis(4-(*N*-phenyl-*N*-(4-methylphenyl)amino)phenyl)-2,1,3-benzothiadiazole<sup>11</sup> (MTPABT, λ<sub>abs</sub> = 465 nm) was also supplied. We can see that the absorption spectrum of TPB3 overlaps with the PL spectrum of PF better than that of MTPABT, favoring more efficient Förster energy transfer from PF host to TPB3 in PL and EL process.

Figure 2 shows the highest occupied molecular orbital (HOMO) and lowest unoccupied molecular orbital (LUMO) energy levels of TPB3 and PF. Both of the HOMO/LUMO energy levels of TPB3 are located between the HOMO/LUMO energy levels of PF, indicating effective charge trapping in the EL process. TPB3 also exists good thermal properties with a high glass transition temperature (*T*<sub>g</sub>) of 162 °C and thermal decomposition temperature (*T*<sub>d</sub>) of 605 °C, which further guarantee their thermal stability in EL devices.

TABLE 1 Photophysical, Electrochemical, and Thermal Properties of TPB3

	λ <sub>abs</sub> / nm	λ <sub>emi</sub> / nm	Φ <sub>f</sub>	E <sub>onset oxd</sub> / V	E <sub>HOMO</sub> / eV	E <sub>onset red</sub> / V	E <sub>LUMO</sub> / eV	E <sub>g</sub> / eV	T <sub>g</sub> /°C	T <sub>d</sub> /°C
TPB3	452	572	0.79	0.99	-5.33	-1.22	-3.12	2.21	162	605

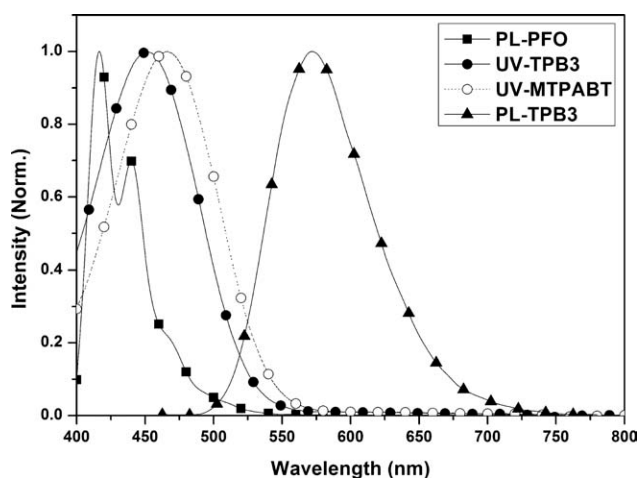


**FIGURE 1** Absorption spectra of TPB3, MTPABT, and PL spectrum of TPB3 in dilute toluene solution.

### Photophysical Properties of the Polymers

Figure 3 shows the absorption spectra of S-WP-003TPB3 and PL spectra of all the polymers in solid films. Actually, all these polymers exhibit similar absorption spectra to PF with an absorption peak around at 393 nm, ascribed to the  $\pi$ - $\pi^*$  transition of the PF backbones. The absorption of orange dopant at about 452 nm could not be observed because of its extremely low content. The PL spectra of all these polymers in solid films with an excitation wavelength of 380 nm show two emission peaks at around 436 and 560 nm. According to our previous studies,<sup>9–13</sup> the two distinguishable PL peaks of the star-like polymers can be attributed to the individual emissions originating from the PF backbone and the orange dopant units. The orange emission band comes from the Förster energy transfer from PF host to TPB3 dopants due to the spectra overlap between the emission spectrum of PF and absorption spectrum of TPB3 (Fig. 1). The relative intensity of the orange emission increases successively as the amount of orange dopant units in the polymer increases because of the higher extent energy transfer.

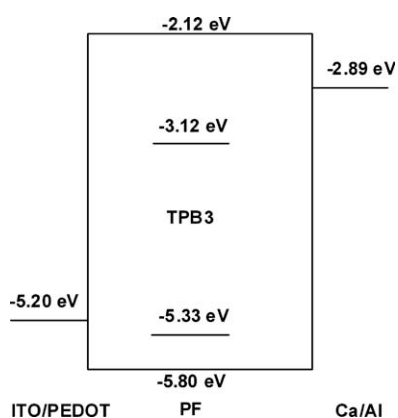


**FIGURE 2** HOMO/LUMO energy levels of TPB3 and PF.

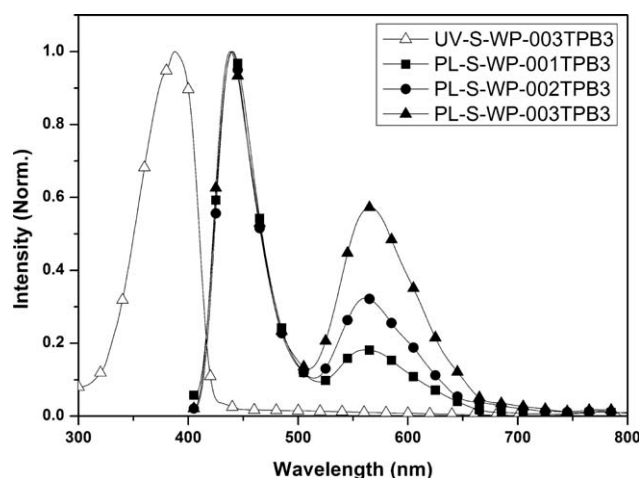


**FIGURE 3** Absorption and PL spectra of the polymers in film.

### EL Performances of the Polymers

To investigate the EL properties of the polymers, single-layer devices [ITO/PEDOT:PSS (40 nm)/polymer (100 nm)/Ca (10 nm)/Al (100 nm)] were fabricated. Here, ITO, PEDOT and PSS respectively stands for indium tin oxide, poly(3,4-ethylenedioxythiophene) and poly(styrenesulfonate). The EL spectra of the devices of these polymers at 7.0 V are shown in Figure 4. The corresponding emission maxima and CIE coordinates are outlined in Table 2. It can be seen that the EL spectra of S-WP-xTPB3 also show two simultaneous blue and orange emission bands with peaks at 424/440 nm and 560 nm, respectively. However, comparing PL (Fig. 3) and EL (Fig. 4) spectra, we note that the relative intensity of orange peaks in the EL spectra is significantly higher than that of the PL spectra of the same polymer composition. It seems that, in EL process, direct charge trapping might also play an important role besides the Förster energy transfer process from PF host to orange dopants, resulting in enhanced orange emission.

The EL performances of the devices of S-WP-xTPB3 are also demonstrated in Table 2. The LE-current density curves of

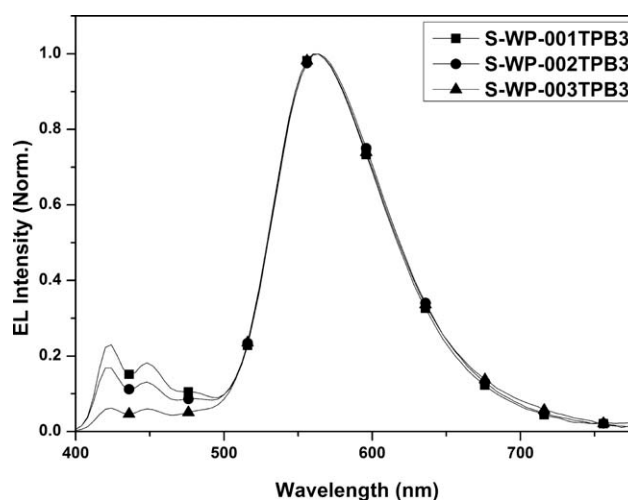


**FIGURE 4** EL spectra of the pristine polymers at 7.0 V.

**TABLE 2** EL Performance of the Pristine Device of S-WP-xTPB3

	Von (V)	LE (cd A <sup>-1</sup> )	PE (lm W <sup>-1</sup> )	Brightness (cd m <sup>-2</sup> )	EQE (%)	λ <sub>max</sub> (nm)	CIE/ (x, y)
S-WP-001TPB3	4.5	9.61	6.04	9139	3.21	424/448/560	(0.41, 0.48)
S-WP-002TPB3	5.0	12.96	6.51	12270	4.29	424/448/560	(0.42, 0.49)
S-WP-003TPB3	5.0	15.27	9.48	15470	4.93	424/448/560	(0.45, 0.51)

the PLEDs are illustrated in Figure 5. In contrast to our previous reports based on linear dopants,<sup>11,23b</sup> the EL efficiency based on the TPB3-containing polymers increase successively with doping concentration. The EL performance is improved from a LE of 9.61 cd A<sup>-1</sup>, a maximum brightness of 9139 cd m<sup>-2</sup> and a maximum EQE of 3.21% for S-WP-001TPB3 to a LE of 15.27 cd A<sup>-1</sup>, a maximum brightness of 15,470 cd m<sup>-2</sup> and a maximum EQE of 4.93% for S-WP-003TPB3. As a result, we realized much more efficient electroluminescence from star-like single-polymer systems compared with linear orange molecule doped polymers. Three considerable factors might contribute to it. First, star-shaped dopant units molecular design strategy is helpful for reducing the dipole-dipole molecular interaction of the dopant units. Second, more PF arms might provide better shield to the dopant cores. Thus, the concentration quenching effect of the dopant units could be further suppressed. Third, compared to MTPABT units, more effective energy transfer from PF host to TPB3 leads to higher EL efficiency of PLEDs (Fig. 1). We found that when the content of TPB3 changed from 0.01 to 0.03 mol %, the turn-on voltage of the device increased a little, probably due to the charge-trapping effect of TPB3 unit.<sup>30</sup>

Although the LE efficiencies of the pristine devices are relatively high, they do not realize white electroluminescence due to the excessive energy transfer from PF host to TPB3 dopant. To obtain white electroluminescence, the devices were thermal annealed at 120 °C for 0.5 h in vacuum box before the Ca/Al cathode was evaporated. The EL spectra of

the annealed devices are shown in Figure 6. We observed that the relative intensity of blue emission of the annealed device is reinforced significantly with red-shifted peak emission at 436/460 nm. As a result, white electroluminescence has been realized for the annealed device of S-WP-002TPB3, with CIE coordinates of (0.33, 0.36).

The absorption spectra of annealed films of these polymer and pristine film of S-WP-003TPB3 are shown in Figure 7a. A new absorption band around 422 nm can be observed due to the formation of α-phase PF.<sup>14b</sup> Based on the relative intensity of this new band, more than 20% α-phase PF was formed.<sup>14b</sup> The α-phase PF induced the enhanced and red-shifted blue emission band in PL spectrum of S-WP-003TPB3 (Fig. 7b), as well as the similar aforementioned phenomena in EL spectra.

The EL performances of the annealed devices of the polymers are listed in Table 3. The EL efficiencies of all the annealed PLEDs are higher than corresponding pristine ones, especially for the EQE values, which improved around 30%. The device of S-WP-002TPB3 realized a comparably high LE of 16.62 cd A<sup>-1</sup> (Fig. 8) at a current density of 22.56 mA cm<sup>-2</sup> with a brightness of 3717 cd m<sup>-2</sup>, which is almost twice that of MTPABT-doped linear polymers. The optimizing mechanism is mainly due to the following four factors. First, the formation of crystalline α-phase PF favors balanced hole and electron transport to improve the light-emitting efficiency.<sup>14a</sup> Second, the generated α-phase PF acts as an electron trap site and self-dopant.<sup>31</sup> It allows efficient charge trapping and energy transfer to occur. Thus, the charge recombination

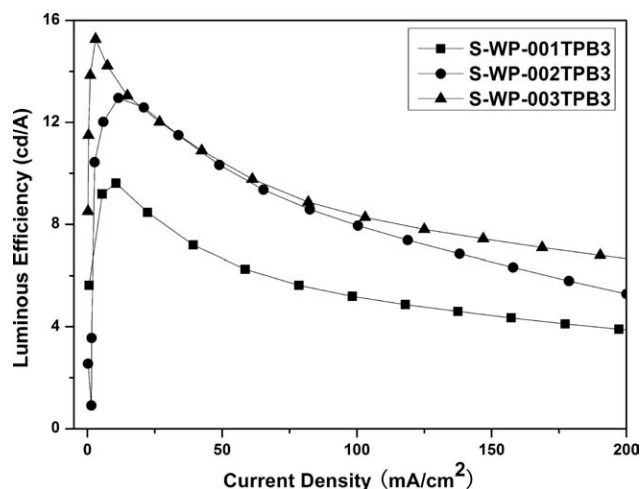


**FIGURE 5** Luminous efficiency-current density curves of the pristine devices.

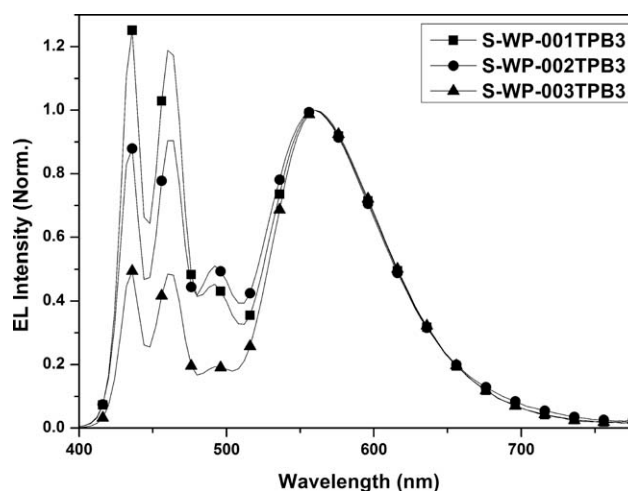


**FIGURE 6** EL spectra of the annealed polymers at 7.0 V.

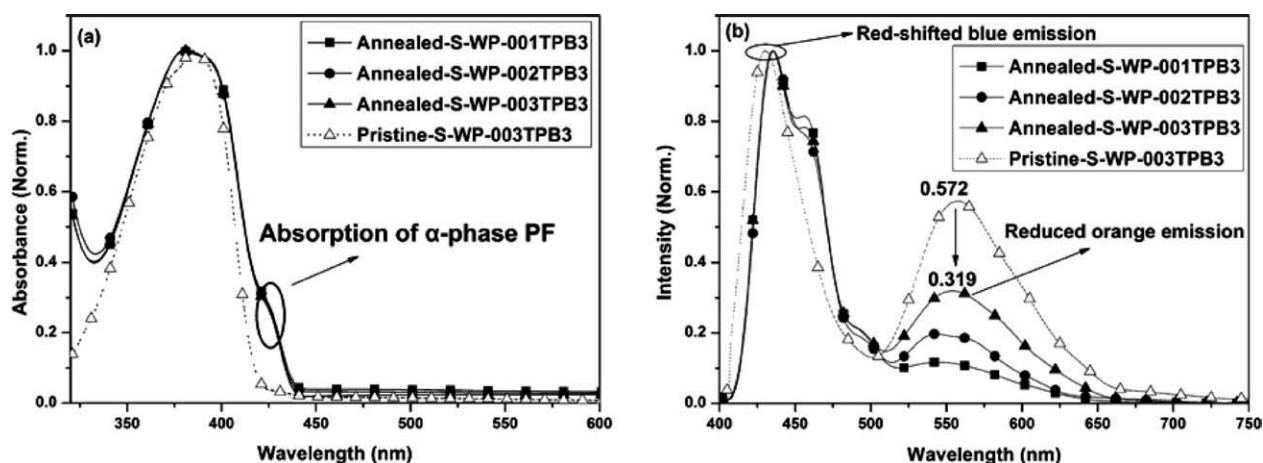


FIGURE 7 Absorption spectra (a) and PL spectra of annealed polymers in film state.

efficiency and the radiative decay efficiency of polymer systems are improved. Third, red-shifted blue emission with stronger human eye response benefits for higher LE and PE. Fourth, the content of  $\alpha$ -phase PF in polymer is so high (around 20%) that it actually serves as an assistant-dopant<sup>32</sup> for orange dopant as well, which leads to the cascade energy transfer<sup>33</sup> from amorphous PF through  $\alpha$ -phase PF to orange dopants. As a result, more efficient energy transfer from blue host to orange dopant and superior device efficiency were achieved. The turn-on voltage of the annealed devices increases about 1.0 V compared to the pristine ones because of the charge-trapping effect of  $\alpha$ -phase PF.

## EXPERIMENTAL

### Materials

4,7-Dibromo-2,1,3-benzothiadiazole<sup>34</sup> (**1**), tributyl(4-(*N*-phenyl-*N*-(4-methylphenyl)amino)phenyl)stannane<sup>11</sup> (**2**), 1,3,5-tris(4-(boronic acid)phenyl)benzene<sup>27</sup> (**3**), 2-bromo-7-(trimethyleneborate)-9,9-dioctylfluorene<sup>23b</sup> (**4**) were synthesized as literatures.

### 4-(4-(*N*-Phenyl-*N*-(4-methylphenyl)amino)phenyl)-7-bromo-2,1,3-benzothiadiazole (**5**)

A mixture of 4,7-dibromo-2,1,3-benzothiadiazole (**1**) (2.85 g, 9.71 mmol), tributyl(4-(*N*-phenyl-*N*-(4-methylphenyl)amino)phenyl)stannane (**2**) (2.67 g, 4.86 mmol), Pd(PPh<sub>3</sub>)<sub>4</sub> (0.04 mg, 0.04 mmol), and toluene (40 mL) was kept stirred under argon in the dark at 100 °C for 24 h. After cooling, the solution was stirred in saturated aqueous potassium fluoride for 3 h, then extracted with dichloromethane, washed with water and dried with anhydrous Na<sub>2</sub>SO<sub>4</sub>. The crude product was purified

with silica column chromatography (eluent: petroleum ether/CH<sub>2</sub>Cl<sub>2</sub> 2:1) and recrystallized in petroleum ether/CH<sub>2</sub>Cl<sub>2</sub> mixed solvents to afford a yellow solid. Yield: 1.55 g (68.3%). <sup>1</sup>H NMR (CDCl<sub>3</sub>, 300 MHz)  $\delta$  (ppm): 7.92 (d, 1H), 7.81 (d, 2H), 7.56 (d, 1H), 7.30 (t, 2H), 7.20–7.09 (m, 8H), 7.07 (t, 3H), 2.37 (s, 3H). MALDI-TOF (Matrix-assisted laser desorption/ionization-time of flight mass spectrometry) (*m/z*): 471.0 [M<sup>+</sup>].

### 1,3,5-Tris(4-(7-(4-(*N*-phenyl-*N*-(4-methylphenyl)amino)phenyl)-2,1,3-benzothiadiazole-4-)phenyl)benzene (TPB3)

A mixture of 1,3,5-tris(4-(boronic acid)phenyl)benzene (**3**) (0.18 g, 0.40 mmol), 4-(4-(*N*-phenyl-*N*-(4-methylphenyl)amino)phenyl)-7-bromo-2,1,3-benzothiadiazole (**5**) (0.62 g, 1.32 mmol), Pd(PPh<sub>3</sub>)<sub>4</sub> (0.02 g, 0.01 mmol), 2 M aqueous K<sub>2</sub>CO<sub>3</sub> (10 mL), Aliquat 336 (0.10 g), and toluene (30 mL) was heated to 100 °C and stirred in dark for 12 h. After workup, the mixture was extracted with CHCl<sub>3</sub>, washed with water and dried with anhydrous Na<sub>2</sub>SO<sub>4</sub>. The residue was purified by column chromatography (eluent: petroleum ether/CHCl<sub>3</sub> 1:1) and recrystallized twice in petroleum ether/CHCl<sub>3</sub> mixed solvents to obtain a yellow solid. Yield: 0.36 g (60.1%). <sup>1</sup>H NMR (CDCl<sub>3</sub>, 300 MHz)  $\delta$  (ppm): 8.14 (d, 6H), 8.01 (s, 3H), 7.93 (d, 6H), 7.91–7.85 (m, 9H), 7.79 (d, 3H), 7.29 (t, 6H), 7.23–7.16 (m, 12H), 7.15–7.09 (m, 12H), 7.05 (t, 3H), 2.35 (s, 9H). <sup>13</sup>C NMR (CDCl<sub>3</sub>, 75 MHz)  $\delta$  (ppm): 154.50, 154.36, 148.05, 147.04, 144.65, 142.31, 141.20, 137.10, 134.21, 133.18, 132.49, 132.45, 131.32, 130.50, 130.31, 130.02, 128.42, 127.85, 127.61, 125.92, 125.70, 125.57, 122.99, 115.36, 21.16. Anal. Calcd. For C<sub>99</sub>H<sub>69</sub>N<sub>9</sub>S<sub>3</sub>: C, 80.30; H, 4.70; N, 8.51; Found: C, 79.92; H, 4.25; N, 8.78. MALDI-TOF (*m/z*): 1479.5 [M<sup>+</sup>].

TABLE 3 EL performance of the annealed device of S-WP-xTPB3

	V <sub>on</sub> (V)	LE (cd A <sup>-1</sup> )	PE (lm W <sup>-1</sup> )	Brightness (cd m <sup>-2</sup> )	EQE (%)	$\lambda_{\max}$ (nm)	CIE (x, y)
S-WP-001TPB3	5.5	11.05	6.03	9624	4.52	436/460/560	(0.29, 0.30)
S-WP-002TPB3	5.8	16.62	7.73	15100	6.28	436/460/560	(0.33, 0.36)
S-WP-003TPB3	6.0	17.86	7.55	16890	6.49	436/460/560	(0.39, 0.45)

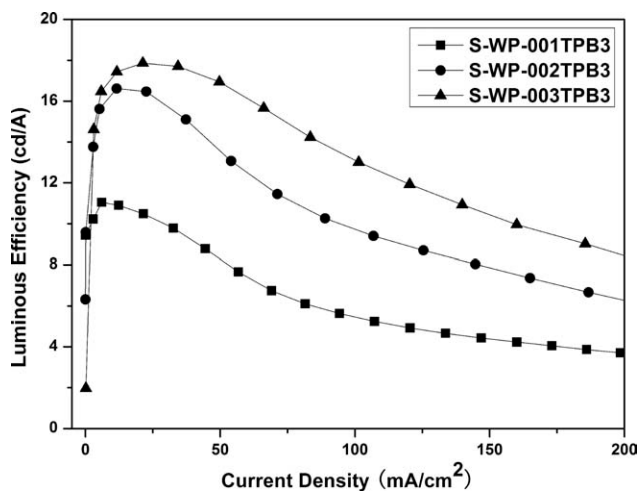


**FIGURE 8** Luminous efficiency–current density curves of the annealed devices of the polymers.

**1,3,5-Tris(4-(7-(4-(N-(4-bromophenyl)-N-(4-methylphenyl)amino)phenyl)-2,1,3-Benzothiadiazole-4-)phenyl)benzene (Mon-TPB3)**

To a solution of TPB3 (0.15 g, 0.10 mmol) in fresh chloroform, tetrabutylammonium tribromide (0.15 g, 0.31 mmol) in chloroform solvent (10 mL) was dropwise added. The mixture was stirred at room temperature for 6 h. Then, it was washed with aqueous sodium hydrogen sulfate and brine followed by drying over anhydrous Na<sub>2</sub>SO<sub>4</sub>. After filtration and removal of the solvent, the residue was purified by flash silica column chromatography (eluent: CHCl<sub>3</sub>) and recrystallized twice in petroleum ether/CHCl<sub>3</sub> mixed solvents to give a yellow solid. Yield: 0.15 g (87.2%). <sup>1</sup>H NMR (CDCl<sub>3</sub>, 300 MHz) δ (ppm): 8.14 (d, 6H), 8.01 (s, 3H), 7.90 (d, 12H), 7.83 (d, 6H), 7.40 (d, 12H), 7.21 (d, 6H), 7.05 (d, 12H), 2.35 (s, 9H). <sup>13</sup>C NMR (CDCl<sub>3</sub>, 75 MHz) δ (ppm): 154.47, 154.34, 148.02, 147.03, 144.64, 142.25, 141.12, 137.05, 134.21, 133.12, 132.50, 132.38, 131.29, 130.52, 130.31, 130.00, 128.40, 127.81, 127.59, 125.93, 125.70, 125.52, 122.96, 115.37, 21.18. Anal. Calcd. For C<sub>99</sub>H<sub>69</sub>Br<sub>3</sub>N<sub>9</sub>S<sub>3</sub>: C, 69.23; H, 3.87; N, 7.34; Found: C, 68.94; H, 4.24; N, 7.69. MALDI-TOF (*m/z*): 1713.2 [M<sup>+</sup>]

**General Procedure of the Polymers**

A mixture of 2-bromo-7-(trimethyleneborate)-9,9-dioctylfluorene (4), Aliquat 336 (0.10 g, 0.25 mmol), Pd(PPh<sub>3</sub>)<sub>4</sub> (0.01 g, 0.01 mmol) under argon was added degassed toluene solution of orange dopant Mon-TPB3 with corresponding feed ratios, 2 M aqueous K<sub>2</sub>CO<sub>3</sub> (2 mL) and degassed toluene (6 mL in total). The resulting mixture was stirred in the dark at 90 °C for 48 h, and then sequentially end-capped with 0.1 M phenylboronic acid (2 mL) and bromobenzene (1 mL), stirring for 12 h for each addition. After cooling, the reaction mixture was poured into methanol and filtered. The precipitate was collected and dissolved in dichloromethane, washed with water and dried with anhydrous Na<sub>2</sub>SO<sub>4</sub>. After evaporating most of the solvent, the residue was precipitated in stirred methanol solvent to give a fiber-like solid. The polymer was further purified by Soxhlet extraction with

acetone for 24 h. The reprecipitation procedure in dichloromethane-methanol was then repeated several times. The final product was obtained after drying in vacuum with a yield of 60–70%.

**PF:** light yellow fiber. *M<sub>n</sub>* = 7.43 × 10<sup>4</sup>, PDI = 2.25

**S-WP-001TPB3:** orange fiber. *M<sub>n</sub>* = 8.21 × 10<sup>4</sup>, PDI = 2.28

**S-WP-002TPB3:** orange fiber. *M<sub>n</sub>* = 7.95 × 10<sup>4</sup>, PDI = 2.32

**S-WP-003TPB3:** orange fiber. *M<sub>n</sub>* = 7.28 × 10<sup>4</sup>, PDI = 2.34

As previous single-polymers reported in our group, all these polymers exhibits similar <sup>1</sup>H NMR and elemental analysis results as those of PF due to the low content of orange dopant units: <sup>1</sup>H NMR (CDCl<sub>3</sub>, 300 MHz) δ (ppm): 7.87 (d, 2H), 7.72 (br, 4H), 2.10 (br, 4H), 1.14 (br, 24H), 0.81 (t, 6H). Anal. Calcd: C, 89.69; H, 10.31. Found: C, 89.08; H, 10.02.

**Measurement and Characterization**

<sup>1</sup>H NMR spectra were recorded with a Bruker AV300 NMR spectrometer. The elemental analyses were performed using a Bio-Rad elemental analysis system. MALDI-TOF was measured by a Bruker Daltonics Flexanalysis system. The number- and weight-average molecular weights of the polymers were determined by gel permeation chromatography (GPC) using a Waters 410 instrument with polystyrene as standard and THF as eluent. UV-Vis absorption spectra were measured by a Perkin-Elmer Lambda 35 UV/Vis spectrometer. PL spectra were recorded by a Perkin-Elmer LS50B spectrofluorometer. The relative fluorescent quantum yields of TPB3 in toluene solution were measured as literature<sup>35</sup> using Nile Red in 1,4-dioxane (0.68) as the standard compound. Cyclic voltammograms of polymer films on glassy carbon electrodes were recorded on an EG&G 283 (Princeton Applied Research) potentiostat/galvanostat system at room temperature in a solution of *n*-Bu<sub>4</sub>NClO<sub>4</sub> (0.10 M) in fresh CH<sub>2</sub>Cl<sub>2</sub> at a scan rate of 100 mV s<sup>-1</sup>. A Pt wire and an Ag/AgCl electrode were used as the counter electrode and the reference electrode, respectively. Thermal properties were measured using a Perkin-Elmer TGA-7 thermogravimetric analyzer and a Perkin-Elmer DSC-7 differential scanning calorimeter under nitrogen with a heating rate of 10 °C min<sup>-1</sup>. The EL spectra and current-voltage and brightness-voltage characteristics of the devices were measured in air with a Spectrascan PR650 spectrophotometer in the forward direction and a computer-controlled Keithley 2400 instrument. The EQE values were calculated from the brightness, current density, and EL spectrum, assuming a Lambertian distribution.

**Device Fabrication**

ITO glass plates were degreased in an ultrasonic acetone solvent bath and then dried in a heating chamber at 120 °C. The PEDOT:PSS was spin-coated on the cleaned ITO at 3000 rpm for 60 s and then baked for 20 min at 120 °C to give an approximate thickness of 40 nm. The polymer layer (~ 100 nm) was then spin-coated on to the PEDOT/ITO coated glass substrate in fresh toluene solution (around 15 mg mL<sup>-1</sup>) under ambient atmosphere. Finally, a thin layer of calcium (10 nm) followed by a layer of aluminum (100 nm) was

deposited in a vacuum thermal evaporate or through a shadow mask at a pressure of  $3 \times 10^{-3}$ – $5 \times 10^{-3}$  Pa. The active area of the diodes was about 12 mm<sup>2</sup>. For the annealed device, after emitting polymer layer was spin coated on the PEDOT:PSS layer, the devices were annealed at 120 °C for 30 min and then cooled for 30 min in vacuum box before evaporating the Ca/Al cathode.

## CONCLUSIONS

In summary, by introduction of star-shaped orange dopant to building star-like polymers with three PF arms, the problem of concentration quenching effect in PLEDs based on single-polymer systems was avoided, and highly efficient PLEDs have been realized. Furthermore, through optimizing the devices with thermal annealing treatment to generate self-doping  $\alpha$ -phase PF, we achieved white electroluminescence with reinforced and red-shifted blue emission, balanced charge transport, and superior energy transfer from blue host to orange dopant. As a result, WPLEDs has been achieved with a high LE of 16.62 cd A<sup>-1</sup>, an EQE of 6.28%, and CIE coordinates of (0.33, 0.36). As we know, it is among one of the best results for WPLEDs based on fluorescent polymers.

## ACKNOWLEDGEMENTS

The authors are grateful to the 973 Project (2009CB623601 and 2009CB930603), the Science Fund for Creative Research Groups (No.20921061), and the National Natural Science Foundation of China (Nos. 51173179, 20904055, and 21074130).

## REFERENCES AND NOTES

- (a) Andrade, B. W. D.; Forrest, S. R. *Adv. Mater.* **2004**, *16*, 1585–1595; (b) Sun, Y. R.; Giebink, N. C.; Kanno, H.; Ma, B. W.; Thompson, M. E.; Forrest, S. R. *Nature* **2006**, *440*, 908–912; (c) Raja, I. U. H.; Lee, J. Y.; Kim, I. T.; Lee, S. H. *Monatsh Chem.* **2008**, *139*, 725–738; (d) Reineke, S.; Lindner, F.; Schwartz, G.; Seidler, N.; Walzer, K.; Lüssem, B.; Leo, K. *Nature* **2009**, *459*, 234–238; (e) Wu, H. B.; Ying, L.; Yang, W.; Cao, Y. *Chem. Soc. Rev.* **2009**, *38*, 3391–3400; (f) Ulbricht, C.; Beyer, B.; Friebe, C.; Winter, A.; Schubert, U. S. *Adv. Mater.* **2009**, *21*, 4418–4441; (g) Kamtekar, K. T.; Monkman, A. P.; Bryce, M. R. *Adv. Mater.* **2010**, *22*, 572–582; (h) Wang, Q.; Ma, D. G. *Chem. Soc. Rev.* **2010**, *39*, 2387–2398; (i) Farinola, G. M.; Ragni, R. *Chem. Soc. Rev.* **2011**, *40*, 3467–3482; (j) Wang, R. J.; Liu, D.; Ren, H. C.; Zhang, T.; Yin, H. M.; Liu, G. Y.; Li, J. Y. *Adv. Mater.* **2011**, *23*, 2823–2827.
- (a) Gong, X.; Wang, S.; Moses, D.; Bazan, G. C.; Heeger, A. J. *Adv. Mater.* **2005**, *17*, 2053–2058; (b) Xu, Y.; Peng, J.; Mo, Y.; Hou, Q.; Cao, Y. *Appl. Phys. Lett.* **2005**, *86*, 163502; (c) Zhou, Y.; Sun, Q.; Tan, Z.; Zhong, H.; Yang, C.; Li, Y. *J. Phys. Chem. C* **2007**, *111*, 6862–6287.
- (a) Berggen, M.; Inganäs, O.; Gustafsson, G.; Rasmusson, J.; Andersson, M. R.; Hjertberg, T.; Wennerström, O. *Nature* **1994**, *372*, 444–446; (b) Kido, J.; Shionoya, H.; Nagai, K. *Appl. Phys. Lett.* **1995**, *67*, 2281–2283; (c) Granström, M.; Inganäs, O. *Appl. Phys. Lett.* **1996**, *68*, 147–149; (d) Hu, B.; Karasz, F. E. *J. Appl. Phys.* **2003**, *93*, 1995–2001; (e) Gong, X.; Ma, W. L.; Ostrowski, J. C.; Bazan, G. C.; Moses, D.; Heeger, A. J. *Adv. Mater.* **2004**, *16*, 615–619; (f) Xu, Q. F.; Duong, H. M.; Wudl, F.; Yang, Y. *Appl. Phys. Lett.* **2004**, *85*, 3357–3359; (g) Kim, J. H.; Herguth, P.; Kang, M. S.; Jen, A. K. Y. *Appl. Phys. Lett.* **2004**, *85*, 1116–1168; (h) Al Attar, H. A.; Monkman, A. P.; Tavasli, M.; Bettington, S.; Bryce, M. R. *Appl. Phys. Lett.* **2005**, *86*, 121101; (i) Sun, Q. J.; Fan, B. H.; Tan, Z. A.; Yang, C. H.; Li, Y. F.; Yang, Y. *Appl. Phys. Lett.* **2006**, *88*, 163510; (j) Shih, P. I.; Tseng, Y. H.; Wu, F. I.; Dixit, A. K.; Shu, C. F. *Adv. Funct. Mater.* **2006**, *16*, 1582–1589; (k) Kim, T. H.; Lee, H. K.; Park, O. O.; Chin, B. D.; Lee, S. H.; Kim, J. K. *Adv. Funct. Mater.* **2006**, *16*, 611–617; (l) Shih, P. I.; Shu, C. F.; Tung, Y. L.; Chi, Y.; *Appl. Phys. Lett.* **2006**, *88*, 251110.
- (a) Tsai, M. L.; Liu, C. Y.; Hsu, M. A.; Chow, T. J. *Appl. Phys. Lett.* **2003**, *82*, 550–552; (b) Lee, Y. Z.; Chen, X. W.; Chen, M. C.; Chen, S. A.; Hsu, J. H.; Fann, W. S. *Appl. Phys. Lett.* **2001**, *79*, 308–310; (c) Paik, K. L.; Baek, N. S.; Kim, H. K.; Lee, J. H.; Lee, Y. *Macromolecules* **2002**, *35*, 6782–6791.
- (a) Huang, J.; Li, G.; Wu, E.; Xu, Q.; Yang, Y. *Adv. Mater.* **2006**, *18*, 114–117; (b) Huang, J.; Hou, W. J.; Li, J. H.; Li, G.; Yang, Y. *Appl. Phys. Lett.* **2006**, *89*, 133509.
- Zou, J. H.; Liu, J.; Wu, H. B.; Peng, J. B.; Yang, W.; Cao, Y. *Org. Electron.* **2009**, *10*, 843–848.
- (a) Huang, F.; Shih, P. I.; Shu, C. F.; Chi, Y.; Jen, A. K. Y. *Adv. Mater.* **2009**, *21*, 361–365; (b) Wu, H. B.; Zhou, G. J.; Zou, J. H.; Ho, C. L.; Wong, W. Y.; Yang, W.; Peng, J. B.; Cao, Y. *Adv. Mater.* **2009**, *21*, 4181–4184; (c) Cheng, G.; Fei, T.; Duan, Y.; Zhao, Y.; Ma, Y. Y.; Liu, S. Y. *Opt. Lett.* **2010**, *35*, 2436–2438; (d) Zou, J. H.; Wu, H.; Lam, C. S.; Wang, C. D.; Zhu, J.; Zhong, C. M.; Hu, S. J.; Ho, C. L.; Zhou, G. J.; Wu, H. B.; Choy, W. C. H.; Peng, J. B.; Cao, Y.; Wong, W. Y. *Adv. Mater.* **2011**, *23*, 2976–2980.
- Wu, H. B.; Zou, J. H.; Liu, F.; Wang, L.; Mikhailovsky, A.; Bazan, G. C.; Yang, W.; Cao, Y. *Adv. Mater.* **2008**, *20*, 696–702.
- (a) Tu, G. L.; Mei, C. Y.; Zhou, Q. G.; Cheng, Y. X.; Geng, Y. H.; Wang, L. X.; Ma, D. G.; Jing, X. B.; Wang, F. S. *Adv. Funct. Mater.* **2006**, *16*, 101–106; (b) Liu, J.; Zhou, Q. G.; Cheng, Y. X.; Geng, Y. H.; Wang, L. X.; Ma, D. G.; Jing, X. B.; Wang, F. S. *Adv. Mater.* **2005**, *17*, 2974–2978.
- Tu, G. L.; Zhou, Q. G.; Cheng, Y. X.; Wang, L. X.; Ma, D. G.; Jing, X. B.; Wang, F. S. *Appl. Phys. Lett.* **2004**, *85*, 2172–2174.
- Liu, J.; Zhou, Q. G.; Cheng, Y. X.; Geng, Y. H.; Wang, L. X.; Ma, D. G.; Jing, X. B.; Wang, F. S. *Adv. Funct. Mater.* **2006**, *16*, 957–965.
- (a) Liu, J.; Guo, X.; Bu, L. J.; Xie, Z. Y.; Cheng, Y. X.; Geng, Y. H.; Wang, L. X.; Jing, X. B.; Wang, F. S. *Adv. Funct. Mater.* **2007**, *17*, 1917–1925; (b) Liu, J.; Xie, Z. Y.; Cheng, Y. X.; Geng, Y. H.; Wang, L. X.; Jing, X. B.; Wang, F. S. *Adv. Mater.* **2007**, *19*, 531–535.
- (a) Liu, J.; Shao, S. Y.; Chen, L.; Xie, Z. Y.; Cheng, Y. X.; Geng, Y. H.; Wang, L. X.; Jing, X. B.; Wang, F. S. *Adv. Mater.* **2007**, *19*, 1859–1863; (b) Liu, J.; Chen, L.; Shao, S. Y.; Xie, Z. Y.; Cheng, Y. X.; Geng, Y. H.; Wang, L. X.; Jing, X. B.; Wang, F. S. *Adv. Mater.* **2007**, *19*, 4224–4228.
- (a) Niu, X. D.; Qin, C. J.; Zhang, B. H.; Yang, J. W.; Xie, Z. Y.; Wang, L. X.; Jing, X. B.; Wang, F. S. *Appl. Phys. Lett.* **2007**, *90*, 203513; (b) Zhang, B. H.; Qin, C. J.; Ding, J. Q.; Chen, L.; Xie, Z. Y.; Cheng, Y. X.; Wang, L. X. *Adv. Funct. Mater.* **2010**, *20*, 2951–2957.
- (a) Jiang, J.; Xu, Y.; Yang, W.; Guan, R.; Liu, Z.; Zhen, H.; Cao, Y. *Adv. Mater.* **2006**, *18*, 1769–1773; (b) Luo, J.; Li, X.; Hou, Q.; Peng, J.; Yang, W.; Cao, Y. *Adv. Mater.* **2007**, *19*, 1113–1117.
- (a) Wu, F. I.; Yang, X. H.; Neher, D.; Dodda, R.; Tseng, Y. H.; Shu, C. F. *Adv. Funct. Mater.* **2007**, *17*, 1085–1092; (b) Chuang, C. Y.; Shih, P. I.; Chien, C. H.; Wu, F. I.; Shu, C. F. *Macromolecules* **2007**, *40*, 247–252; (c) Chien, C. H.; Shih, P. I.; Shu, C. F. *J. Polym. Sci. Part A: Polym. Chem.* **2007**, *45*, 2938–2946.

- 17** (a) Lee, S. K.; Hwang, D. H.; Jung, B. J.; Cho, N. S.; Lee, J.; Lee, J. D.; Shim, H. K. *Adv. Funct. Mater.* **2005**, *15*, 1647–1655; (b) Lee, S. K.; Jung, B. J.; Ahn, T. Y.; Jung, K.; Lee, J. I.; Kang, I. N.; Lee, J.; Park, J. H.; Shim, H. K. *J. Polym. Sci. Part A: Polym. Chem.* **2007**, *45*, 3380–3388; (c) Lee, S. K.; Ahn, T.; Cho, N. S.; Lee, J. I.; Jung, Y. K.; Lee, J.; Shim, H. K. *J. Polym. Sci. Part A: Polym. Chem.* **2007**, *45*, 1199–1209.
- 18** (a) Lee, P. I.; Hsu, S. L. C.; Lee, R. F. *Polymer* **2007**, *48*, 110–115; (b) Lee, P. I.; Hsu, S. L. C.; Lee, J. F. *J. Polym. Sci. Part A: Polym. Chem.* **2008**, *46*, 464–472; (c) Lee, P. I.; Hsu, S. L. C.; Lin, P. Y. *Macromolecules* **2010**, *43*, 8051–8057.
- 19** Wu, W. C.; Lee, W. Y.; Chen, W. C. *Macromol. Chem. Phys.* **2006**, *207*, 1131–1138.
- 20** Lin, Z. H.; Lin, Y. D.; Wu, C. Y.; Chow, P. T.; Sun, C. H.; Chow, T. J. *Macromolecules* **2010**, *43*, 5925–5931.
- 21** Chien, C. H.; Liao, S. F.; Wu, C. H.; Shu, C. F.; Chang, S. Y.; Chi, Y.; Chou, P. T.; Lai, C. H. *Adv. Funct. Mater.* **2008**, *18*, 1430–1439.
- 22** Chen, C. T. *Chem. Mater.* **2004**, *16*, 4389–4400.
- 23** (a) Liu, J.; Chen, L.; Shao, S. Y.; Xie, Z. Y.; Cheng, Y. X.; Geng, Y. H.; Wang, L. X.; Jing, X. B.; Wang, F. S. *J. Mater. Chem.* **2008**, *18*, 319–327; (b) Liu, J.; Cheng, Y. X.; Xie, Z. Y.; Geng, Y. H.; Wang, L. X.; Jing, X. B.; Wang, F. S. *Adv. Mater.* **2008**, *20*, 1357–1362.
- 24** (a) Li, B. S.; Li, J.; Fu, Y. Q.; Bo, Z. S. *J. Am. Chem. Soc.* **2004**, *126*, 3430–3431; (b) Li, B. S.; Xu, X. J.; Sun, M. H.; Fu, Y. Q.; Yu, G.; Liu, Y. Q.; Bo, Z. S. *Macromolecules* **2006**, *39*, 456–461; (c) Pei, J.; Wang, J. L.; Cao, X. Y.; Zhou, X. H.; Zhang, W. B. *J. Am. Chem. Soc.* **2003**, *125*, 9944–9945; (d) Cao, X. Y.; Zhang, W. B.; Wang, J. L.; Zhou, X. H.; Lu, H.; Pei, J. *J. Am. Chem. Soc.* **2003**, *125*, 12430–12431; (e) Lin, W. J.; Chen, W. C.; Wu, W. C.; Niu, Y. H.; Jen, A. K. Y. *Macromolecules* **2004**, *37*, 2335–2341.
- 25** Lai, W. Y.; Xia, R. D.; He, Q. Y.; Levermore, P. A.; Huang, W.; Bradley, D. D. C. *Adv. Mater.* **2009**, *21*, 355–360.
- 26** Chou, C. H.; Hsu, S. L.; Dinakaran, K.; Chiu, M. Y.; Wei, K. H. *Macromolecules* **2005**, *38*, 745–751.
- 27** Chen, L.; Li, P. C.; Cheng, Y. X.; Xie, Z. X.; Wang, L. X.; Jing, X. B.; Wang, F. S. *Adv. Mater.* **2011**, *23*, 2986–2990.
- 28** Thomas, K. R. J.; Lin, J. T.; Velusamy, M.; Tao, Y. T.; Cheun, C. H. *Adv. Funct. Mater.* **2004**, *14*, 83–90.
- 29** Scherf, U.; List, E. J. W. *Adv. Mater.* **2002**, *14*, 477–487.
- 30** (a) Utsugi, K.; Yakano, S. *J. Electrochem. Soc.* **1992**, *139*, 3610–3615; (b) Uchida, M.; Adachi, C.; Koyama, T.; Taniguchi, Y. *J. Appl. Phys.* **1999**, *86*, 1680–1687.
- 31** Lu, H. H.; Liu, C. Y.; Chang, C. H.; Chen, S. A. *Adv. Mater.* **2007**, *19*, 2574–2579.
- 32** (a) Hamada, Y.; Kanno, H.; Tsujioka, T.; Takahashi, H.; Usuki, T. *Appl. Phys. Lett.* **1999**, *75*, 1682–1684; (b) Feng, J.; Li, F.; Gao, W.; Cheng, G.; Xie, W.; Liu, S. *Appl. Phys. Lett.* **2002**, *81*, 2935–2937.
- 33** Berggren, M.; Dodabalapur, A.; Slusher, R. E.; Bao, Z. *Nature* **1997**, *39*, 466–469.
- 34** Herguth, P.; Jiang, X. Z.; Liu, M. S.; Jen, A. K. Y. *Macromolecules* **2002**, *35*, 6094–6100.
- 35** Eaton, D. F. *Pure Appl. Chem.* **1988**, *60*, 1107–1114.